INTERNATIONAL JOURNAL FOR NUMERICAL METHODS IN FLUIDS
Int. J. Numer. Meth. Fluids 2006; **50**:131–145
Published online 7 September 2005 in Wiley InterScience (www.interscience.wiley.com). DOI: 10.1002/fld.1039

Quadratic programming algorithm for wall slip and free boundary pressure condition

C. W. Wu[1,*,†] and H. X. Sun[2,‡]

[1]*State Key Laboratory of Structural Analysis for Industrial Equipment, Department of Engineering Mechanics, Dalian University of Technology, Dalian 116024, China*
[2]*Department of Science and Technology, Dalian University of Technology, Dalian 116024, China*

SUMMARY

Wall slip is often observed in a highly sheared fluid film in a solid gap. This makes a difficulty in mathematical analysis for the hydrodynamic effect because fluid velocity at the liquid–solid interfaces is not known *a priori*. If the gap has a convergent–divergent wedge, a free boundary pressure condition, i.e. Reynolds pressure boundary condition, is usually used in the outlet zone in numerical solution. This paper, based on finite element method and parametric quadratic programming technique, gives a numerical solution technique for a coupled boundary non-linearity of wall slip and free boundary pressure condition. It is found that the numerical error decreases with the number of elements in a negative power law having an index larger than 2. Our method does not need an iterative process and can simultaneously gives rise to fluid film pressure distribution, wall slip velocity and surface shear stress. Wall slip always decreases the hydrodynamic pressure. Large wall slip even causes a null hydrodynamic pressure in a pure sliding solid gap. Copyright © 2005 John Wiley & Sons, Ltd.

KEY WORDS: wall slip; free boundary; quadratic programming

1. INTRODUCTION

Fluid mechanics is one of the oldest and most useful basic sciences in engineering applications. For hundreds of years it has relied on the assumption that no slip occurs at the interface of liquid and solid, i.e. no relative motion exists between the liquid molecules adjacent to the solid and the solid surface. This is the so-called no-slip boundary condition used in many

*Correspondence to: Chengwei Wu, State Key Laboratory of Structural Analysis for Industrial Equipment, Department of Engineering Mechanics, Dalian University of Technology, Dalian 116024, China.
†E-mail: cwwu@dlut.edu.cn
‡E-mail: cindyhxsun@yahoo.com

Contract/grant sponsor: Natural Science Foundation of China; contract/grant numbers: 10272028, 10332010
Contract/grant sponsor: Specialized Research Fund for the Doctoral Program of Higher Education; contract/grant number: 20030141013
Contract/grant sponsor: Excellent Young Teachers Program

Received 30 January 2005
Revised 19 May 2005
Accepted 23 May 2005

textbooks of fluid mechanics and is applied successfully to many engineering areas. However, is the no-slip boundary condition always correct and reliable? The answer is no. In fact, this success cannot reflect the accuracy of the boundary condition but may reflect the insensitivity of an experiment to the partial-slip boundary condition, as stated by Craig *et al.* [1].

During recent years it has been found that wall slip (or boundary slip) often occurs in the flow of a polymer melt [2, 3]. More recently, many experiments observed that wall slip of a liquid occurs not only at a poorly wetting surface [1, 4–7], but also in a wetting surface [8–10]. Although many possible mechanisms for wall slip have been proposed, the experimental manifestation of wall slip is the existence of a critical or limiting wall-shear stress. When the surface shear stress is below the limiting shear stress no slip occurs. When the surface shear stress reaches the limiting value, however, a slip occurs. In lubrication mechanics, if the lubricant has a limiting shear yield stress, for example a viscoplastic fluid [11, 12], wall slip will occur at wall–lubricant interfaces when the wall shear stress is sufficiently high. Wu *et al.* [13, 14] found that a hydrodynamic failure may happen for a slider bearing lubricated with a viscoplastic fluid at a high shear rate.

In numerical analysis of a wall slip problem, the wall slip cannot be known *a priori*. This makes for difficulty in the numerical process, especially when wall slip and free boundary pressure condition are coupled together. Stahl and Jacobson [15], using a difference method, gave a full numerical solution for elastohydrodynamic lubrication of line contact. Huang *et al.* [16] and Spikes [17] analysed wall slip occurring at a slider bearing also using a difference method. In all the numerical analyses of difference methods, several possibilities of wall slip have to be listed. In the numerical solution process, an iterative process has to be used and often has problems converging to a solution [15]. Strozzi [18] gave an early concept to analyse one wall slip using a complementarity method. This method needs not an iterative process, but it dealt with only a very special wall slip (known inlet volume flow and the slip occurring at only one surface) and cannot be used to address engineering applications. This paper presents a general numerical method for the numerical solution of wall slip and free boundary pressure condition using a finite element method together with a quadratic programming technique. The wall slip can take place at one or both of the solid surfaces.

2. MATHEMATICAL ANALYSIS METHOD

2.1. Control equations for wall slip

Based on parametric variational principle described in Reference [14] for a viscoplastic lubrication of a slider bearing, the wall slips coupled with free boundary pressure condition are studied in the present paper. The lubricant velocities at surfaces a and b, $\bar{u}_a$ and $\bar{u}_b$, can be expressed by (see Figure 1)

$$\bar{u}_\alpha = u_\alpha + u_\alpha^{\mathrm{s}} \quad (\alpha = a, b) \tag{1}$$

where u_a and u_b denote the velocities of solid surfaces a and b, respectively, and u_a^{s} and u_b^{s} are the corresponding wall slip velocities. In the lubrication mechanics of fluid film, it is assumed that the fluid film thickness in the studied domain is so small than the size of the lubricated surface that the fluid velocity component in y direction can be neglected [19]. Thus the fluid

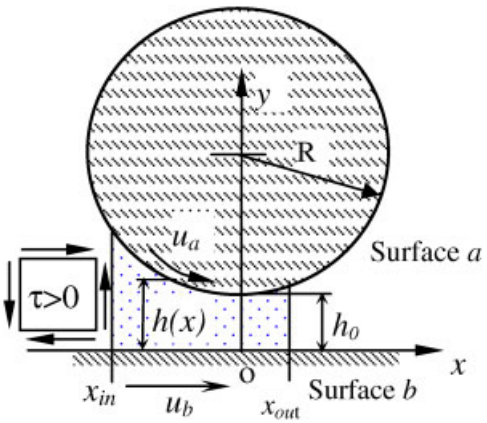

Figure 1. Schematic of fluid flow in a thin gap between a roller and a plane.

absolute velocity equals approximately its component in x direction. If $u_\alpha^s > 0$ $(\alpha = a, b)$ wall slip goes in the positive x direction. Otherwise it goes in the negative x direction.

Using the yield function concept in elasto-plastic structural analysis, the slip functions for wall slip can be written as

$$f(\tau_\alpha, p) = |\tau_\alpha| - \tau_{L\alpha} \leqslant 0, \quad (\alpha = a, b) \tag{2}$$

where τ is the shear stress at solid–lubricant interface, p the film pressure, τ_L the limiting shear stress at the interface, and the subscript α denotes the surface a or b (see Figure 1). The limiting shear stress is given by Bair and Winer [11] as

$$\tau_{L\alpha} = \tau_{0\alpha} + k_\alpha p, \quad (\alpha = a, b) \tag{3}$$

where $\tau_{0\alpha}$ is the initial shear strength when the film pressure equals zero, and k_α is a constant of proportionality. Consequently, the slip function (2) can be rewritten as

$$f_\alpha^{(1)} = \tau_\alpha - (\tau_{0\alpha} + k_\alpha p) \leqslant 0, \quad (\alpha = a, b) \tag{4a}$$

$$f_\alpha^{(2)} = -\tau_\alpha - (\tau_{0\alpha} + k_\alpha p) \leqslant 0, \quad (\alpha = a, b) \tag{4b}$$

The sign of the wall slip velocity has the following relationships with surface shear stress: $\text{sign}(u_a^s) = -\text{sign}(\tau_a)$ and $\text{sign}(u_b^s) = \text{sign}(\tau_b)$. Consequently, the slip velocities can be given by

$$u_a^s = \{-1, 1\}\{\lambda_a^{(1)}, \lambda_a^{(2)}\}^T \tag{5a}$$

$$u_b^s = \{1, -1\}\{\lambda_b^{(1)}, \lambda_b^{(2)}\}^T \tag{5b}$$

where $\lambda_a^{(1)}$ and $\lambda_a^{(2)}$ denote, respectively, the absolute values of wall slip velocities in negative x and positive x directions at surface a, but $\lambda_b^{(1)}$ and $\lambda_b^{(2)}$ denote, respectively, the absolute

values of wall slip velocities in positive x and negative x directions at surface b. They have the relationship: $\lambda_\alpha^{(1)} \bullet \lambda_\alpha^{(2)} = 0$, $\lambda_\alpha^{(i)} \geqslant 0$ $(i = 1,2;\ \alpha = a,b)$. The shear stresses at surfaces a and b can be written as

$$\tau_a = \frac{h}{2}\frac{\partial p}{\partial x} + \frac{u_a - u_b}{h}\eta + \frac{u_a^{\mathrm{s}} - u_b^{\mathrm{s}}}{h}\eta \tag{6a}$$

$$\tau_b = -\frac{h}{2}\frac{\partial p}{\partial x} + \frac{u_a - u_b}{h}\eta + \frac{u_a^{\mathrm{s}} - u_b^{\mathrm{s}}}{h}\eta \tag{6b}$$

where h is the fluid film thickness and η the fluid viscosity. Substituting Equations (6a), (6b) and (5a), (5b) into Equations (4a) and (4b), the slip control equations can be written as

$$f_\alpha^{(i)}(p, \partial p/\partial x, h, \lambda_a, \lambda_b) + v_\alpha^{(i)} = 0 \tag{7a}$$

$$\lambda_\alpha^{(i)} \cdot v_\alpha^{(i)} = 0, \quad \lambda_\alpha^{(i)} \geqslant 0, \quad v_\alpha^{(i)} \geqslant 0 \quad (i = 1,2; \alpha = a,b) \tag{7b}$$

where $v_\alpha^{(i)}$ are the slack variables complementary to the control variables $\lambda_\alpha^{(i)}$. If $f_\alpha^{(i)} < 0$, then $\lambda_\alpha^{(i)} = 0$ $(i = 1,2;\ \alpha = a,b)$, which indicates no wall slip occurs. If $f_\alpha^{(i)} = 0$, then $\lambda_\alpha^{(i)} > 0$ $(i = 1,2;\ \alpha = a,b)$, which indicates that a wall slip occurs. No case of $f_\alpha^{(i)} > 0$ will take place.

2.2. *Finite element formulation*

Assume that the moving velocity of the plane is along ox-axis (see Figure 1), the Reynolds equation with wall slip for constant viscosity and isothermal lubrication is [19]

$$\frac{\partial}{\partial x}\left(\frac{h^3}{12\eta}\frac{\partial p}{\partial x}\right) - \frac{1}{2}\frac{\partial}{\partial x}[h(u_a + u_b + u_a^{\mathrm{s}} + u_b^{\mathrm{s}})] = 0 \tag{8}$$

The corresponding variational functional is [14, 20]

$$J(p) = \int_{x_{\mathrm{in}}}^{x_{\mathrm{out}}} \left[\frac{h^3}{24\eta}\left(\frac{\partial p}{\partial x}\right)^2 - \frac{h}{2}(u_a + u_b + u_a^{\mathrm{s}} + u_b^{\mathrm{s}})\frac{\partial p}{\partial x}\right] \mathrm{d}x + q_{\mathrm{s}} p_{\mathrm{s}} \tag{9}$$

where x_{in} and x_{out} are the locations of the inlet and outlet coordinates of the studied domain of fluid film, respectively, q_{s} the known boundary volume flow (negative when it flows into the studied fluid domain and positive when it flows out of the domain), and p_{s} the corresponding unknown film pressure. It is assumed that the lubricated region is divided into m finite elements with n nodes. Also it is assumed that $\lambda_\alpha^{(i)}$, which characterizes slip state, is constant in an element.

Because fluid cannot resist large tensile stress, it is generally assumed that a negative film pressure is impossible. In other words, the variational functional (9) should have $p \geqslant 0$ as an additional constraint to Equations (7a) and (7b). Consequently, the problem mentioned above

can be summarized as the following discrete optimization problem:

$$\text{Min}\, J(p) = \tfrac{1}{2}\{p\}[K]\{p\} - \{p\}^{\mathrm{T}}([B](\{u_a\} + \{u_b\}) + [\Phi]\{\lambda\} - \{q\}) - \{\mu\}^{\mathrm{T}}\{p\} \tag{10a}$$

$$\text{s.t. } [C]\{p\} - [M]\{\lambda\} + \{d\} - \{v\} = 0 \tag{10b}$$

$$\lambda_j v_j = 0, \quad \lambda_j \geqslant 0, \quad v_j \geqslant 0, \quad (j = 1, 2, \ldots\ldots, m-1, m) \tag{10c}$$

$$\mu_j p_j = 0, \quad p_j \geqslant 0, \quad \mu_j \geqslant 0, \quad (j = 1, 2, \ldots\ldots, n-1, n) \tag{10d}$$

where $\{\mu\}$ is the Lagrangian multiplier vector. Letting $\delta J(p)/\delta p = 0$ in Equation (10a) and making use of Equations (10b)–(10d), the following complementary problem is obtained:

$$[K]\{p\} - ([B](\{u_a\} + \{u_b\}) + [\Phi]\{\lambda\} - \{q\}) - \{\mu\} = 0 \tag{11a}$$

$$[C]\{p\} - [M]\{\lambda\} + \{d\} - \{v\} = 0 \tag{11b}$$

$$\lambda_j v_j = 0, \quad \lambda_j \geqslant 0, \quad v_j \geqslant 0, \quad (j = 1, 2, \ldots\ldots, m-1, m) \tag{11c}$$

$$\mu_j p_j = 0, \quad p_j \geqslant 0, \quad \mu_j \geqslant 0, \quad (j = 1, 2, \ldots\ldots, n-1, n) \tag{11d}$$

The problem described by Equations (11a)–(11d) can be solved by many methods. In the present paper the Lemke method is used [21]. After we get the solution, the Reynolds boundary condition can be automatically satisfied.

3. FLUID FLOW IN A SLIDING GAP WITH ONE WALL SLIP

In order to show the feasibility and reliability of our method, first we analysed the same example as given by Strozzi [18]. Strozzi studied one wall slip problem of a slider bearing with a constant inlet volume flow. In the slider bearing shown in Figure 2(a), the upper surface is stationary, but the lower surface moves at a speed $u_b = 0.4\,\text{m/s}$. The following data are used: $h_{\text{in}} = 2\,\text{mm}$, $h_{\text{out}} = 1\,\text{mm}$, $B = 1\,\text{m}$, $\eta = 0.125\,\text{Pa s}$, $k_a = k_b = 0$, which are all the same as those used in Reference [18]. The boundary conditions are $p = 0$ at $x = B$ and the inlet volume flow per unit width $q_{\text{in}} = 0.266667 \times 10^{-3}\,\text{m}^3/\text{s}$ at $x = 0$, which is the volume inflow of an otherwise similar slider bearing, but in the absence of slippage and with null boundary pressures. Suppose that $\tau_{0a} \gg \tau_{0b}$, slip can occur only at the lower surface. Therefore, the slip control equations at surface a can be removed. Now let us analyse the slip problems when $\tau_{0b} = 30, 40$ and $50\,\text{Pa}$, respectively.

The computed results are in good agreement with those given in Reference [18], see Figures 2(a)–(c). Two hundred linear elements (201 nodes) are used in this calculation while 100 nodes were used in the difference solution of Strozzi [18]. When $\tau_{0b} = 50\,\text{Pa}$, no wall slip occurs. When $\tau_{0b} = 40\,\text{Pa}$, partial slip takes place on over 61% of the lower surface in the left side. When $\tau_{0b} = 30\,\text{Pa}$, over 77% of the lower surface has wall slip. With decrease in the limiting shear stress, larger and larger a wall slip takes place on the left side of the lower surface, where the surface shear stress reaches its limiting value (see Figure 2(b)). The

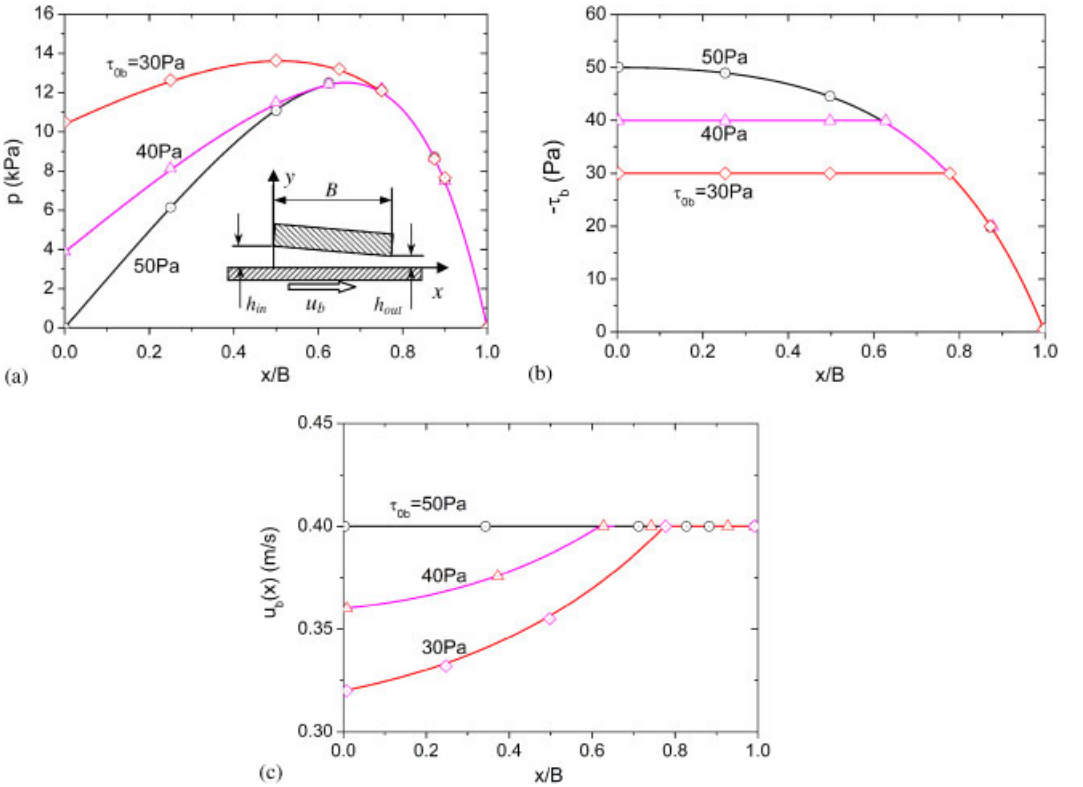

Figure 2. One wall slip analysis with a constant inlet volume flow ($q_{\text{in}} = 0.266667\ \text{m}^3/\text{s}$) boundary condition at $x = 0$ and $p = 0$ at $x = B$ for three surface limiting shear stresses $\tau_{0b} = 50, 40$ and 30 Pa: (a) fluid pressure distribution; (b) shear stress of fluid at lower surface b; and (c) fluid velocity at lower surface. The open symbols are predicted by Strozzi [18]: $\odot$ $\tau_{0b} = 50\,\text{Pa}$, $\triangle$ $\tau_{0b} = 40\,\text{Pa}$, $\diamond$ $\tau_{0b} = 30\,\text{Pa}$.

maximum amplitude of wall slip occurs at the inlet position ($h = h_{\text{in}}$, see Figure 2(c)). All the slips on the lower surface occur in the negative x direction.

In order to show accuracy of the present method, Figure 3 gives the computation error with an increase in the number of uniform finite elements when the limiting shear stress of lower surface $\tau_{0b} = 40\,\text{Pa}$. The computation value at $m = 800$ is considered as the true value. Computation error for each parameter is defined as the relative error of the calculated value and that obtained when $m = 800$. For example, the computation error for load support w is defined as $w_{\text{err}} = |w_{800} - w_m|/w_{800}$, where the subscript 800 and m denote, respectively, the number of elements to be 800 and m. It can be found that, with an increase in the number of elements, the computation errors decrease in a manner of negative power. For the fluid load support w, its computational error gives approximately $w_{\text{err}} = 7/m^{2.2}$. When the number of elements $m = 100$, the computed error for w is decreased to less than 0.03%. It should be pointed out that this numerical example has not yet a true analytical solution. Only Strozzi's numerical result is available to compare. Our numerical results show that after the number of elements is greater than 500, the computed fluid load support capacity changes less than

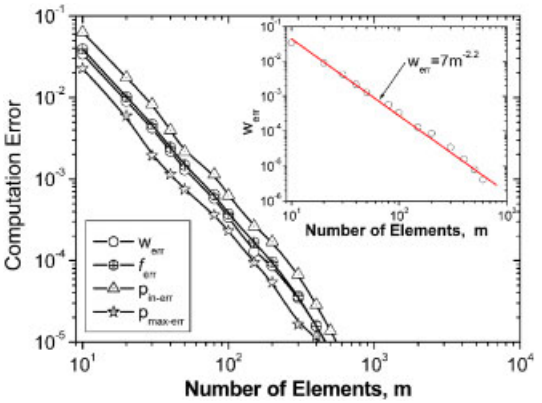

Figure 3. Computational errors for the indicated parameters, where w is the fluid load support, f the friction force at lower surface, p_{in} the inlet pressure, or the pressure at the first node, $p_{\max}$ the maximum pressure, and m the number of elements. The subscript err denotes the computational error for the corresponding parameter.

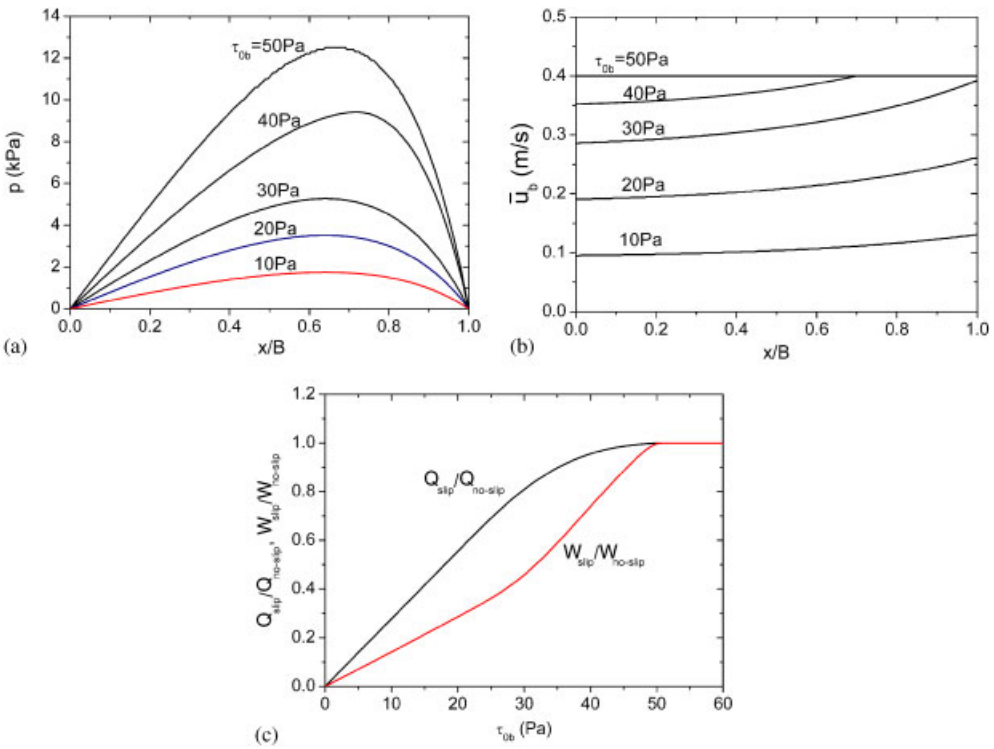

Figure 4. One wall slip analyses with null pressure boundary conditions for several limiting shear stresses at lower surface: (a) fluid pressure distribution; (b) fluid velocity at lower surface; and (c) ratios of fluid load support and volume flow with and without slip. m=200, u_b=0.4 m/s, u_a=0,η=0.125 Pa s, $h_{\text{in}} = 2$ mm, $h_{\text{out}} = 1$ mm, $B = 1$ m.

0.001%. However, our numerical solution for the load support capacity in the case of no slip gives rise to an error of 0.004% compared with the analytical solution (actual solution) when the number of elements $m = 200$.

Figure 4 gives the wall slip analysis with null pressure boundary conditions ($p = 0$ at $x = 0$ and $p = 0$ at $x = B$) for several limiting shear stresses at the lower surface. As contrasted with those shown in Figure 2, the fluid pressure, fluid flow volume and the load support all decrease with the surface limiting shear stress. After the surface limiting shear stress $\tau_{0b} \leqslant 30$ Pa, slip occurs over all of the lower surface. It can be seen that wall slip dramatically reduces the hydrodynamic load support capacity of a fluid film flowing at a wedge gap. The volume flow past the sliding gap is also decreased with the wall slip occurring at the moving surface.

4. FLUID FLOW IN A CONVERGENT–DIVERGENT WEDGE

Now we study the hydrodynamic response of fluid confined between two curved solid surfaces with relative motion. Any two curved surfaces with curvature radii R_1 and R_2 in a non-conforming contact can be approximated by a curved surface with curvature $R = R_1R_2/(R_1 + R_2)$ and a plane, as shown in Figure 1. The following dimensionless parameters are used: $P = pR/(\eta U)$, $T_{0\alpha} = \tau_{0\alpha}R/(\eta U)$, $T_{L\alpha} = \tau_{L\alpha}R/(\eta U)$, $T_\alpha = \tau_\alpha R/(\eta U)$, $Q = q/(UR)$, $W = w/(\eta U)$, where $U = u_a + u_b$, $U_a = u_a/U$, $U_b = u_b/U$, $\alpha = a, b$. The fluid film thickness, as shown in Figure 1, can be written approximately as [19]

$$h(x) = h_0 + x^2/2R \tag{12}$$

where h_0 is the minimum film thickness at $x = 0$ and R is the roller radius.

In the numerical simulations the following parameters are used: $h_0/R{=}10^{-5}$, $x_{in}/R{=}-0.2$, $x_{out}/R{=}0.01$. First we study the wall slip occurring at a pure sliding motion ($U_a{=}1, U_b{=}0$). It is assumed that the lower surface (stationary) has a surface limiting shear strength ($T_{0b}{=}2 \times 10^5$, $k_b{=}0$) high enough to hold the no-slip condition. Pressure boundary condition at inlet is $p = 0$ at $x/R = -0.2$. At outlet it is a free boundary pressure condition (Reynolds pressure boundary condition), i.e. $p = 0$ and $\partial p/\partial x = 0$ at an unknown position somewhere. The dimensionless limiting shear stress at the upper surface (roller surface) is taken as $T_{0a} = 2 \times 10^4$, so that a wall slip occurs. This is a combination of wall slip and free boundary pressure condition. The fluid pressure and wall slip in the thin fluid film confined between curved surfaces concentrates mostly in the left side of the contact centre. In order to improve the numerical accuracy, 200 non-uniform meshes are used. Small sizes of meshes are employed in the small left zone of the centre. Figure 5(a) gives the fluid film pressure distribution for several values of k_a when the solid surfaces have a pure sliding motion. It can be found that the hydrodynamic pressure concentrates mostly near the small centre zone and we need only to study a small domain of the fluid film. This supports again the assumption of velocity component made in Section 2.1 and the fluid film thickness approximation of Equation (12). Our numerical method needs not an iterative process for such a complex non-linear problem. Reynolds pressure boundary condition was automatically satisfied together with the solution of fluid pressure, wall slip velocity and surface shear stress. Evident is the dramatic drop of fluid pressure due to the large wall slip at small values of k_a. Changes of the fluid flow velocities at upper surface caused by wall slip are shown in Figure 5(b). Wall slip velocities at the centre zone for small values of $k_a \leqslant 0.001$ are so high that the fluid flow velocities at upper surface is

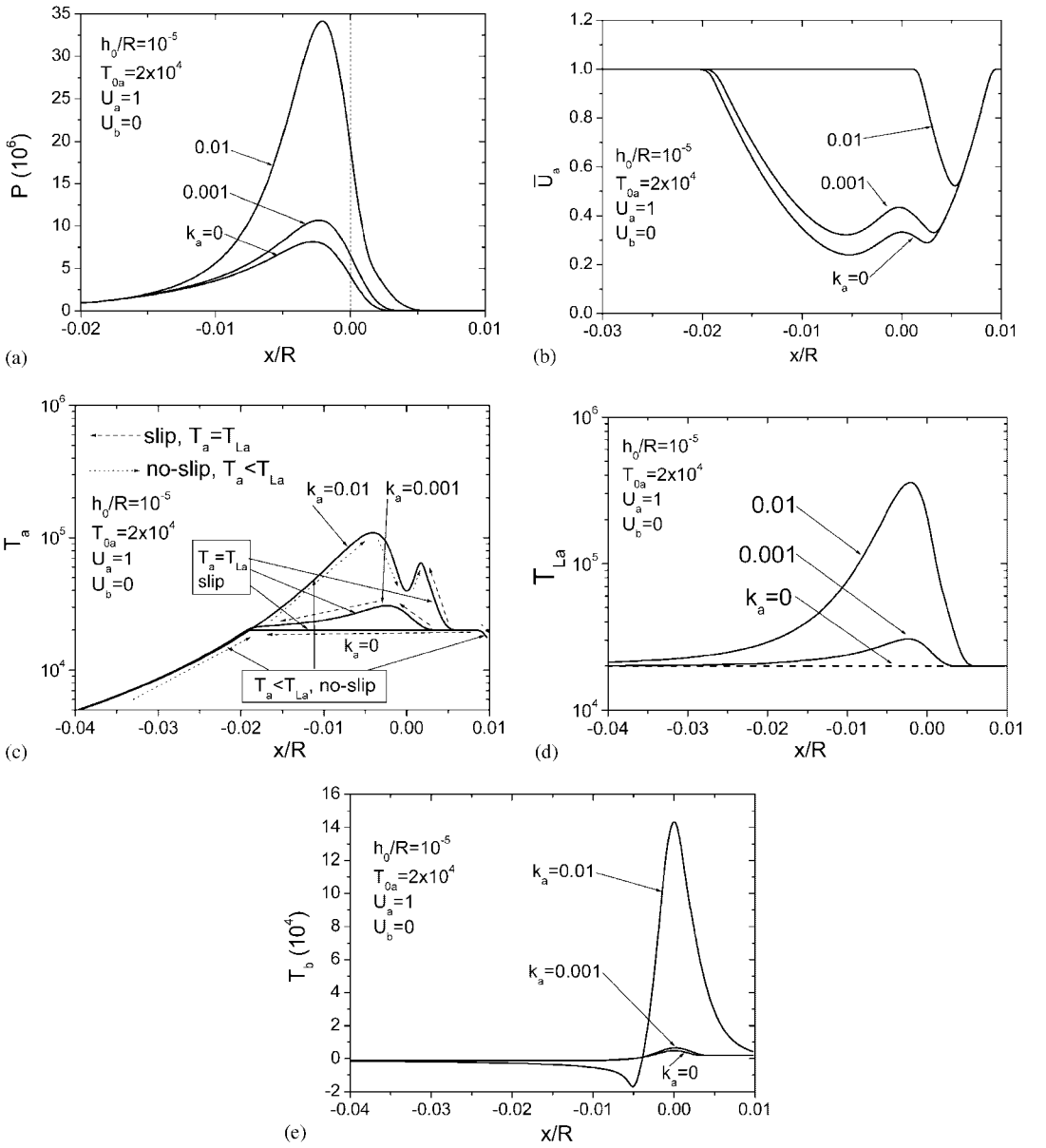

Figure 5. Wall slip analyses at a pure sliding gap given in dimensionless parameters: (a) fluid film pressure distribution for several values of k_a; (b) changes of the fluid velocities at upper surface caused by wall slip; (c) shear stress of fluid film at upper surface; (d) surface limiting shear stress at upper surface; and (e) the surface shear stresses at lower surface. $h_0/R = 10^{-5}$, $U_a = 1$, $U_b = 0$, $T_{0b} = 2 \times 10^5$, $k_b = 0$.

decreased by about 60–75%. The shear stress and limiting shear stress of fluid film at upper surface are given in Figures 5(c) and (d), respectively. Here we can see more clearly how wall slip to develop at upper surface. Wall slip first to be developed in the large pressure gradient region, where a high surface shear stress is easily generated. No wall slip occurs at the regime where the surface shear stress is below its critical value. Figure 5(e) shows the surface shear stress at lower surface, which is smaller than its limiting shear stress. Therefore, no slip occurs at lower surface. Similarly, the surface shear stresses at lower surface after $k_a \leqslant 0.001$ are very small compared with that of $k_a = 0.01$.

Figure 6 gives the numerical results of slip analysis when the two surfaces with a pure sliding motion have the same surface limiting shear stress, i.e. $u_a > 0$, $u_b = 0$, $T_{0a} = T_{0b}$, and $k_a = k_b$. Here we keep $k_a = k_b = 0.01$ and investigate the effect of the dimensionless initial limiting shear stress, $T_{0a}(T_{0b})$, on the wall slip and hydrodynamics of the fluid film. If $T_{0a} = T_{0b} = 10^5$, no slip occurs at any surface and the pressure distribution is the same as that predicted by the classical Reynolds theory. However, if $T_{0a} = T_{0b} = 10^4$ and 5×10^3, a slip occurs at lower surface (stationary) in the outlet zone, but no slip exhibits at upper surface (moving). When $T_{0a} = T_{0b} = 10^3$, slips occur at both surfaces. The fluid pressure decreases dramatically with an increase in wall slip. Finally, the hydrodynamic effect totally disappears.

Figure 7 gives the numerical results of slip analysis when the two surfaces with a pure rolling motion ($u_a = u_b$) have the same surface limiting shear stress. The hydrodynamic effect in a pure rolling condition is stronger than that in a pure sliding condition as shown in Figure 6 if the sum of u_a and u_b is kept as a constant. A considerable hydrodynamic response still exhibits even when the surface dimensionless initial shear strength $T_{0a}(T_{0b})$ is very small (see Figure 7(a)). Only when $T_{0a} = T_{0b} = 0$, does the hydrodynamic effect totally disappear. The fluid velocity at the liquid–solid interface is not a constant but varies with surface property and geometry position (see Figure 7(b)). Comparing Figure 7 with Figure 6, we can see that hydrodynamic response in a pure rolling motion is much better than that in a pure sliding motion in the case of wall slip. This can explain why a scuffing damage may be easy to occur

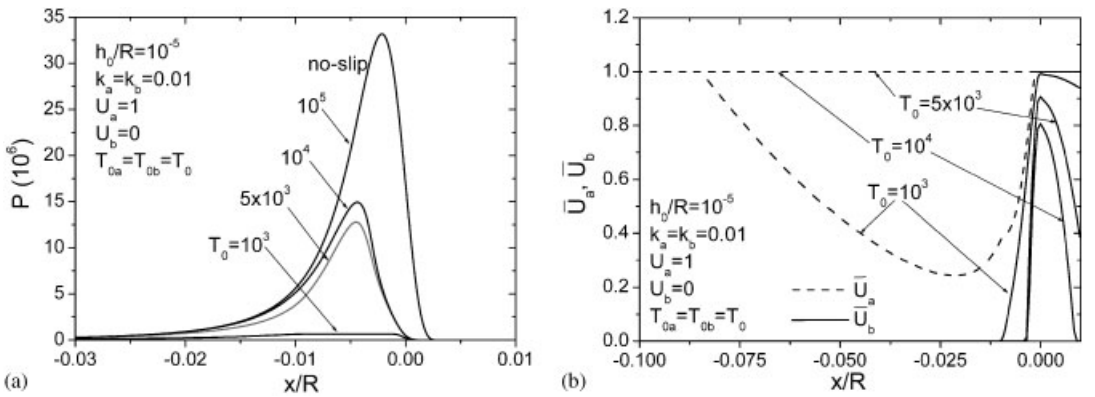

Figure 6. Numerical results of slip analysis for two surfaces in a pure sliding motion given in dimensionless parameters: (a) hydrodynamic fluid pressure; and (b) fluid velocities at solid surfaces. $h_0/R = 10^{-5}$, $U_a = 1$, $U_b = 0$, $k_a = k_b = 0.01$, $T_{0a} = T_{0b} = T_0$.

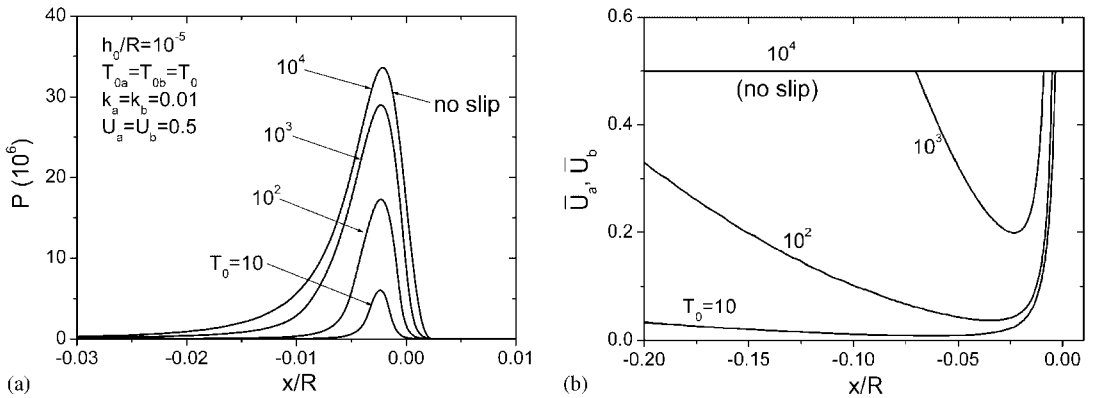

Figure 7. Numerical results of slip analysis for two surfaces in a pure rolling motion given in dimensionless parameters: (a) hydrodynamic fluid pressure; and (b) fluid velocities at solid surfaces ($\bar{U}_a = \bar{U}_b$). $h_0/R = 10^{-5},\ u_a = u_b,\ k_a = k_b = 0.01,\ T_{0a} = T_{0b} = T_0$.

in a pure sliding lubricated contact pair having same material surfaces. But scuffing does not so easily occur in a pure rolling system.

5. DISCUSSIONS

Interfacial limiting shear stress depends on surface roughness, wettability of the surface, fluid viscosity, etc. [6–8, 22]. It can range from the order of 0.1 Pa to the order of MPa [11, 12, 22, 23]. Usually, high viscosity fluid and poor surface wettability easily give rise to a large wall slip. The roughness effect on wall slip is still unclear so far. Zhu and Granick [7] showed that surface nanoroughness reduces wall slip and finally the no-slip boundary condition holds. But Bonaccurso *et al.* [8] reported that surface nanoroughness increases the wall slip. In the present paper, we did not consider the roughness effect. The limiting shear stresses used from Figures 2–4 are just for the purpose of comparison with Strozzi's numerical results [18]. The values of the dimensionless limiting shear stresses used from Figures 5–7 are based on the existing experimental data. For example, if we take $R = 0.1$ m, $U = 1$ m/s and $\eta = 0.01$ Pa s, the limiting shear stress ranges from 1 to 10^4 Pa, giving the corresponding dimensionless limiting shear stress, T_0, ranging from 10 to 10^5.

In a special fluid film studied, the possible slip direction somewhere may be determined previously. In this way the number of control equations described in Equation (7) can be reduced greatly, i.e. the size of matrixes [C], [M] and [Φ] can be reduced. One of the questions in which one is interested may be the computational time of our method. The computational time varies greatly with the studied system and the slip zone size. For example, if we use 200 linear elements, about 10 s are needed for the numerical solution of a single wall slip problem using all the 200 slip control equations at surface b, but about 20 s are needed for wall slip analysis of both surfaces using all the 400 slip control equations, including the input and output process (Pentium IV, 2.8 GHz, 512 M memory). In fact, the slip control equations employed can be reduced according to the possible slip directions. Therefore, the computational time can be further reduced.

6. SUMMARY AND CONCLUSIONS

When a fluid flows in a thin gap between two solid surfaces with relative motion, high hydrodynamic pressure and shear rate may be developed in the fluid film. Wall slip is often observed in such a high sheared fluid film, for example, in thin film lubrication, nanorheology, micro-channel flow and a micro–electro–mechanical-system (MEMS). Wall slip makes a difficulty in mathematical analysis for the hydrodynamic effect because fluid velocity at the liquid–solid interfaces is not known *a priori*. When two close solid surfaces have a relative motion (either tangential or normal direction or both), the fluid confined between them will give a hydrodynamic pressure. If the gap confining fluid has a convergent–divergent wedge and the solid surfaces have a relative tangential motion, Reynolds pressure boundary condition, a typical free boundary pressure condition, is usually used in the outlet zone in numerical solution. One of the most widely used numerical methods to deal with such a free boundary condition is an iterative solution technique.

There are only a few numerical analyses reported so far for wall slip problem based on difference method and iterative solution process. The iterative solution is a tedious process and often has problems converging to a solution with a satisfactory accuracy. For example, the iterative process sometimes is diverging but not converging to a solution. This paper, based on finite element method and parametric quadratic programming technique, gives a numerical solution technique for coupled boundary non-linearity of wall slip and free boundary pressure condition. Our method does not need an iterative process and can simultaneously give rise to fluid pressure distribution, wall slip velocity and surface shear stress. The Reynolds pressure boundary condition can be automatically satisfied in the solution process. It is found that the numerical error decreases with number of elements in a negative power law having an index larger than 2. Numerical solutions show that wall slip first to be developed in the large pressure gradient region, where a high surface shear stress is easily generated, and then the slip region is enlarged with the increase in the relative sliding velocity of solid surfaces. Wall slip dramatically affects generation of the hydrodynamic pressure and always decreases the hydrodynamic pressure. Large wall slip even causes a null hydrodynamic pressure in a pure sliding gap. A better hydrodynamic response is given in a pure rolling motion gap than in a pure sliding gap in the case of wall slip.

NOMENCLATURE

Symbols

A_e	length of element
B	width of slider bearing
f	slip function
h	fluid film thickness
h_0	minimum fluid film thickness
$J(p)$	functional symbol
k	proportional constant
m	number of elements
n	number of nodes

p	film pressure
p_s	film pressure corresponding to q_s
q_s	known boundary volume flow
q	volume flow
R	roller radius
τ	shear stress
τ_L	limiting shear stress
τ_0	initial shear strength
η	fluid viscosity
u	fluid velocity
x	coordinate
y	ordinate
$\bar{u}_a, \bar{u}_b$	fluid velocities at surfaces a and b
u_a, u_b	velocities of surfaces a and b
u_a^s, u_b^s	slip velocities at surfaces a and b
U	$u_a + u_b$
w	fluid film load support
$\lambda_\alpha^{(i)}$	control variable or absolute wall slip velocity
$V_\alpha^{(i)}$	slack variable
[ ]	matrix symbol
{ }	column or row vector symbol

Dimensionless parameters

P	$pR/(\eta U)$
$T_{0\alpha}$	$\tau_{0\alpha}R/(\eta U)$
$T_{L\alpha}$	$\tau_{L\alpha}R/(\eta U)$
T_α	$\tau_\alpha R/(\eta U)$
W	$w/(\eta U)$
Q	$q/(RU)$
U_α	u_α/U
$\bar{U}_\alpha$	$\bar{u}_\alpha/U$

Sub- and Superscripts

α	a, b indicating surface a and b
in, out	inlet and outlet positions of fluid film
e	the eth element
i	1, 2
j	$1,2,\ldots\ldots, m$; or $= 1,2,\ldots\ldots, n$

Matrixes and Vectors

$\mathbf{N}$	interpolation function matrix, $\mathbf{N} = [(x_{e+1} - x)/(x_{e+1} - x_e), (x - x_e)/(x_{e+1} - x_e)]$ $(e = 1,2,3,\ldots,m)$ if a linear element is employed
$\mathbf{u}_{ae}$, $\mathbf{u}_{be}$	solid surface node velocity vectors at the eth element

$\mathbf{f}_\alpha$ $\{f_\alpha^{(1)}, f_\alpha^{(2)}\}^{\mathrm{T}}$

$[K]$ $\sum_{e=1}^{m}\int_{A_e}\frac{h^3}{12\eta}\frac{\partial \mathbf{N}^{\mathrm{T}}}{\partial x}\frac{\partial \mathbf{N}}{\partial x}\,\mathrm{d}x$

$[B]$ $\sum_{e=1}^{m}\int_{A_e}\frac{h}{2}\frac{\partial \mathbf{N}^{\mathrm{T}}}{\partial x}\mathbf{N}\,\mathrm{d}x$

$[\Phi]$ $\sum_{e=1}^{m}\int_{A_e}\frac{h}{2}\left[\frac{\partial \mathbf{N}^{\mathrm{T}}}{\partial x}\{-1,1,1,-1\}\right]\mathrm{d}x$

$[C]$ $\sum_{e=1}^{m}\frac{1}{A_e}\int_{A_e}\left[\frac{h}{2}\left\{-\frac{\partial \mathbf{f}_a^{\mathrm{T}}}{\partial \tau_a},\frac{\partial \mathbf{f}_b^{\mathrm{T}}}{\partial \tau_b}\right\}^{\mathrm{T}}\frac{\partial \mathbf{N}}{\partial x}+\{k_a,k_a,k_b,k_b\}^{\mathrm{T}}\mathbf{N}\right]\mathrm{d}x$

$[M]$ $\sum_{e=1}^{m}\frac{1}{A_e}\int_{A_e}\frac{\eta}{h}\left\{\frac{\partial \mathbf{f}_a^{\mathrm{T}}}{\partial \tau_a},\frac{\partial \mathbf{f}_b^{\mathrm{T}}}{\partial \tau_b}\right\}^{\mathrm{T}}\{-1,1,1,-1\}\,\mathrm{d}x$

$\{d\}$ $\sum_{e=1}^{m}\frac{1}{A_e}\int_{A_e}\left(\{\tau_{0a},\tau_{0a},\tau_{0b},\tau_{0b}\}^{\mathrm{T}}-\frac{\eta}{h}\left\{\frac{\partial \mathbf{f}_a^{\mathrm{T}}}{\partial \tau_a},\frac{\partial \mathbf{f}_b^{\mathrm{T}}}{\partial \tau_b}\right\}^{\mathrm{T}}\mathbf{N}\{\mathbf{u}_{ae}-\mathbf{u}_{be}\}\right)\mathrm{d}x$

$\{p\}$ $\{p_1, p_2, p_3, \ldots, p_n\}^{\mathrm{T}}$

$\{q\}$ $\{-q_{\mathrm{in}}, 0, 0, \ldots, 0\}^{\mathrm{T}}$ if the volume flow is known at the inlet

$\{q\}$ $\{0, 0, \ldots, 0, q_{\mathrm{out}}\}^{\mathrm{T}}$ if the volume flow is known at the outlet

$\{q\}$ $\{0, 0, 0, \ldots, 0\}^{\mathrm{T}}$ if no boundary volume flow condition is given

$\{\lambda\}$ $\{\lambda_{a1}^{(1)}, \lambda_{a1}^{(2)}, \lambda_{b1}^{(1)}, \lambda_{b1}^{(2)}, \ldots, \lambda_{am}^{(1)}, \lambda_{am}^{(2)}, \lambda_{bm}^{(1)}, \lambda_{bm}^{(2)}\}^{\mathrm{T}}$

$\{v\}$ $\{v_{a1}^{(1)}, v_{a1}^{(2)}, v_{b1}^{(1)}, v_{b1}^{(2)}, \ldots, v_{am}^{(1)}, v_{am}^{(2)}, v_{bm}^{(1)}, v_{bm}^{(2)}\}^{\mathrm{T}}$

$\{\mu\}$ $\{\mu_{a1}^{(1)}, \mu_{a1}^{(2)}, \mu_{b1}^{(1)}, \mu_{b1}^{(2)}, \ldots, \mu_{an}^{(1)}, \mu_{an}^{(2)}, \mu_{bn}^{(1)}, \mu_{bn}^{(2)}\}^{\mathrm{T}}$

$\{u_a\}$ $\{u_{a1}\ u_{a2}, \ldots, u_{an}\}^{\mathrm{T}}$

$\{u_b\}$ $\{u_{b1}\ u_{b2}, \ldots, u_{bn}\}^{\mathrm{T}}$

$\sum_{e=1}^{m}$ assembly symbol

ACKNOWLEDGEMENTS

This research was jointly sponsored by the Natural Science Foundation of China (Grant nos. 10272028, 10332010), the Specialized Research Fund for the Doctoral Program of Higher Education (Grant no. 20030141013), and the Excellent Young Teachers Program (EYTP) of Education Ministry of China.

REFERENCES

1. Craig VSJ, Neto C, Williams DRM. Shear-dependent boundary slip in an aqueous Newtonian liquid. *Physical Review Letters* 2001; **87**:054504.
2. Wang SQ. Molecular transitions and dynamics at polymer/wall interfaces: origins of flow instabilities and wall slip. *Advances in Polymer Science* 1999; **138**:227–275.
3. Leger L, Raphael E, Hervet H. Surface-anchored polymer chains: their role in adhesion and friction. *Advances in Polymer Science* 1999; **138**:185–225.
4. Pit R, Hervet H, Leger L. Friction and slip of a simple liquid at solid surface. *Tribology Letters* 1999; **7**: 147–152.
5. Pit R, Hervet H, Leger L. Direct experimental evidence of slip in hexadecane: solid interfaces. *Physical Review Letters* 2000; **85**:980–983.
6. Zhu Y, Granick S. Rate-dependent slip of Newtonian liquid at smooth surfaces. *Physical Review Letters* 2001; **87**:096105.
7. Zhu Y, Granick S. Limits of the hydrodynamic no-slip boundary condition. *Physical Review Letters* 2002; **88**:106102.

8. Bonaccurso E, Butt HJ, Craig VSJ. Surface roughness and hydrodynamic boundary slip of a Newtonian fluid in a completely wetting system. *Physical Review Letters* 2003; **90**:144501.
9. Bonaccurso E, Kappl M, Butt HJ. Hydrodynamic force measurements: boundary slip of hydrophilic surfaces and electrokinetic effects. *Physical Review Letters* 2002; **88**:076103.
10. Kaneta M, Nishikawa N, Kameishi K. Observation of wall slip in elasto-hydrodynamic lubrication. *Journal of Tribology* (ASME) 1990; **112**:447–584.
11. Bair S, Winer WO. Shear strength measurements of lubricants at high pressure. *Journal of Lubrication Technology* (ASME) 1979; **101**:251–256.
12. Bair S, Winer WO. The shear stress rheology of liquid lubricants at pressure of 2 to 200 MPa. *Journal of Tribology* (ASME) 1990; **112**:246–252.
13. Wu CW, Hu LC. Wall slippage and oil film collapse. *Journal of Dalian University of Technology* 1993; **33**(2): 172–178.
14. Wu CW, Zhong WX, Qian LX *et al.* Parametric variational principle for viscoplastic lubrication model. *Journal of Tribology* (ASME) 1992; **113**:731–735.
15. Stahl J, Jacobson BO. A lubricant model considering wall-slip in EHL line contacts. *Journal of Tribology* (ASME) 2003; **125**:523–532.
16. Huang P, Luo JB, Wen SZ. Theoretical study on the lubrication failure of lubricants with a limiting shear stress. *Tribology International* 1999; **32**:421–426.
17. Spikes HA. The half-wetted bearing. Part 1: extended Reynolds equation. *Proceedings of the Institution of Mechanical Engineers Part J*: *Journal of Engineering Tribology* 2003; **217**:1–14.
18. Strozzi A. Formation of three lubrication problems in terms of complementarity. *Wear* 1975; **104**:103–119.
19. Cameron A. *Basic Lubrication Theory* (3rd edn). Ellis Horwood Ltd.: Chichester, U.K., 1981.
20. Huebner KH. *The Finite Element Method for Engineers*. Wiley: New York, 1975.
21. Boot JCG. *Quadratic Programming*: *Algorithms, Anomalies and Applications*. North Holland: Amsterdam, 1964.
22. Granick S, Zhu Y, Lee H. Slippery questions about complex fluids flowing past solids. *Nature Materials* 2003; **2**:221–227.
23. Wu CW, Ma GJ. On the boundary slip of fluid flow. *Science in China G* 2005; **48**(2):178–187.

